

# **J/ $\psi$ measurements in pp and Pb–Pb collisions with the ALICE experiment**

*Cynthia Hadjidakis, for the ALICE Collaboration  
Institut de Physique Nucléaire d'Orsay, Université Paris-Sud, CNRS-IN2P3, Orsay,  
FRANCE*

## **1 Introduction**

The ALICE experiment studies heavy-ion collisions in order to investigate nuclear matter at very high energy density where the formation of a Quark Gluon Plasma (QGP) is expected. Quarkonium production was proposed two decades ago to probe the QGP. It was first predicted that the color-screening of the heavy-quarks potential in deconfined QCD matter would lead to a sequential suppression of the quarkonium states production [1]. Quarkonium production enhancement was also anticipated due to heavy quarks recombination [2]. Measurements carried out at SPS and RHIC [3] revealed a suppression of the J/ $\psi$  (and  $\psi'$  at SPS) production. However it is not clear how to interpret the energy, rapidity and  $p_T$  dependence of the measured suppression. Different effects such as those due to cold (from nuclear initial or final state) or hot nuclear matter may explain the suppression and its kinematical dependence. A new energy regime is opening at the LHC where heavy quarks are produced abundantly. A large production statistics is expected for the J/ $\psi$  and  $\Upsilon$  families, allowing for detailed studies of their production in pp and Pb–Pb collisions. In 2010 and 2011, the LHC provided pp collisions at  $\sqrt{s} = 7$  and 2.76 TeV and Pb–Pb collisions at  $\sqrt{s_{NN}} = 2.76$  TeV per nucleon pair. In this proceeding, we will present published and preliminary results on the measurements of J/ $\psi$  production at mid-rapidity (in the dielectron channel) and at forward rapidity (in the dimuon channel).

## **2 ALICE, A Large Ion Collider Experiment**

ALICE [4] is the LHC experiment dedicated to the study of the heavy-ion collisions. In the central region ( $|\eta| < 0.9$ ), detectors are positioned in a large solenoidal magnet providing an uniform magnetic field of 0.5 T. The main tracking devices consist of the Inner Tracking System (ITS), made of six layers of silicon detectors that surround the beam pipe, and the Time Projection Chamber (TPC), a large cylindrical drift gas detector. In addition, the TPC provides particle identification via the measurement of the specific energy loss  $dE/dx$ . In the forward region ( $-4 < \eta < -2.5$ ), the muon

spectrometer consists of a thick frontal absorber of 10 interaction length ( $\lambda_I$ ), a large 3 T · m dipole magnet, a high granularity tracking system of ten detection planes and a thick muon filter wall ( $7.2 \lambda_I$ ) followed by four planes of trigger chambers. Two forward VZERO scintillator hodoscopes ( $2.8 < \eta < 5.1$  and  $-3.7 < \eta < -1.7$ ) are used for triggering and beam-gas events rejection. Finally, the Zero Degree Calorimeter (ZDC) placed 114 m up- and downstream the Interaction Point allows to reject, in Pb–Pb, electromagnetic interactions and satellite collisions. In pp, the minimum bias trigger (MB) was defined as the logical OR between the requirement of one hit in the ITS pixel layers (SPD), and a signal in one of the two VZERO detectors. The cross sections of the logical AND of the VZERO detectors were measured in pp collisions at 7 TeV and 2.76 TeV [5] and were used for absolute normalisation of the  $J/\psi$  cross section. In Pb–Pb, the logical AND between the ITS pixel layers and the VZERO detectors was used as the MB trigger. For the dimuon analysis, in addition to the MB trigger, a particle that fires the muon trigger system was required.

### 3 Measurements in pp at $\sqrt{s} = 7$ and 2.76 TeV

The results presented here are based on a total integrated luminosity of 5.6 (15.6)  $\text{nb}^{-1}$  in pp collisions at  $\sqrt{s} = 7$  TeV and 1.1 (20)  $\text{nb}^{-1}$  at  $\sqrt{s} = 2.76$  TeV for the dielectron (dimuon) analysis. For the dielectron analysis, the signal is extracted

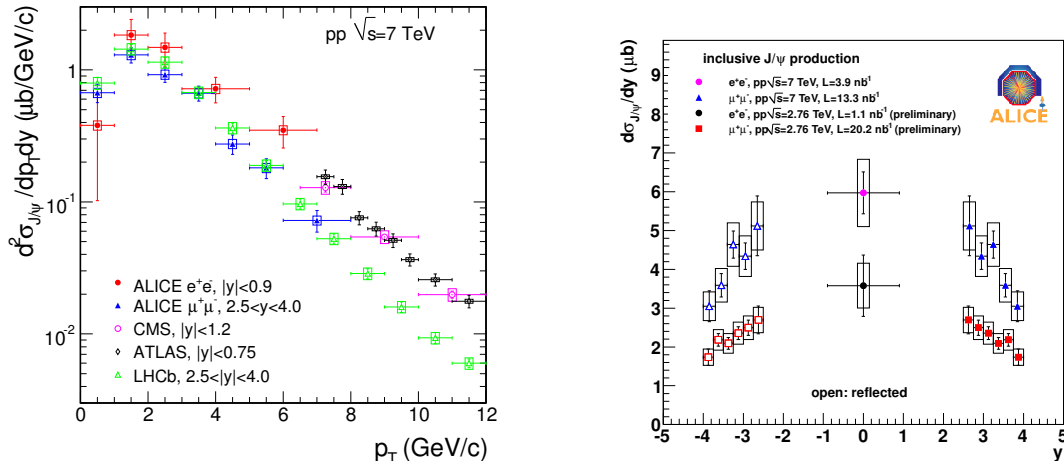


Figure 1: Left:  $J/\psi$   $p_T$ -dependent differential cross sections in pp collisions at 7 TeV [6]. Right:  $y$ -dependent differential cross sections in pp collisions at 7 and 2.76 TeV.

by subtracting the like-sign electron pairs invariant mass distribution normalized to the opposite-sign one outside of the signal region and, for the dimuon analysis, by fitting the opposite-sign muon pairs invariant mass distribution using a Crystal Ball and a double exponential functions. A mass resolution of  $40 \text{ MeV}/c^2$  ( $85 \text{ MeV}/c^2$ )

in the dielectron (dimuon) channel is measured and is well described by detector simulations. The largest systematic uncertainties on the acceptance and cross-section determination arise from the presently unknown value of the  $J/\psi$  polarisation. The total,  $p_T$  and  $y$  differential cross sections were obtained for the inclusive  $J/\psi$  at  $\sqrt{s} = 7$  TeV [6] and at  $\sqrt{s} = 2.76$  TeV [7]. Fig. 1 shows the ALICE  $p_T$ -dependent cross sections at 7 TeV (left) and  $y$ -dependent cross sections at 2.76 and 7 TeV (right). ALICE has a unique coverage at the LHC, allowing to measure the inclusive  $J/\psi$  cross section down to  $p_T=0$  in a large  $y$ -range. A good agreement is found with LHCb (left panel of Fig. 1).  $J/\psi$  production was also measured as a function of the charged particle multiplicity in pp collisions [7]. The  $J/\psi$  polarisation measurement as well as measurements of the fraction of  $J/\psi$  from B mesons decay are being prepared.

## 4 Measurements in Pb–Pb at $\sqrt{s}_{NN} = 2.76$ TeV

Inclusive  $J/\psi$  production was measured in the dielectron and dimuon channels in Pb–Pb collisions. In the dimuon analysis, an integrated luminosity of  $2.7\mu\text{b}^{-1}$  was used. In order to determine the geometry and centrality classes of a Pb–Pb collision, the VZERO amplitude was fitted by a geometrical-Glauber based model [8]. The analysis was limited to the 0-80% most central collisions where the contamination from electromagnetic interactions was estimated to be negligible. Different methods were applied

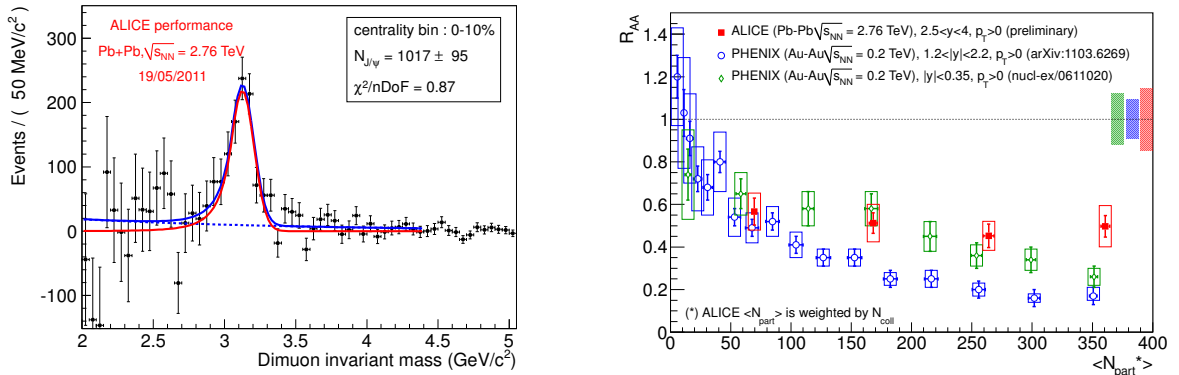


Figure 2: Left: Invariant mass distribution for opposite-sign muon pairs in the centrality class 0-10% after mixed-event combinatorial-background subtraction. Right:  $J/\psi$   $R_{AA}$  as a function of  $\langle N_{part} \rangle$  weighted by  $N_{coll}$ .

to extract the signal. The left part of Fig. 2 shows the invariant mass distribution for opposite-sign muon pairs in the centrality class 0-10% after combinatorial-background subtraction estimated from a mixed-event distribution. The  $J/\psi$  peak is clearly seen in all centrality classes. To measure the nuclear modification factors ( $R_{AA}^i$ ) for a centrality class  $i$ , the  $J/\psi$  yield was normalized to the inclusive  $J/\psi$  cross-section

measured in pp collisions scaled by the corresponding nuclear overlap function ( $T_{AA}^i$ ) calculated using the Glauber model [8]. The signal extraction and the pp reference cross-section uncertainties represent the largest contributions to the  $R_{AA}$  systematic uncertainty. The right plot of Fig. 2 shows  $R_{AA}$  (down to  $p_T=0$ ) as a function of the average number of participant nucleons ( $N_{part}$ ) for ALICE and is compared to the PHENIX results at  $\sqrt{s_{NN}}=200$  GeV. In our measurement, a significant weaker centrality dependence is seen as well as a larger  $R_{AA}$  for the most central collisions. Charm statistical recombination in a QGP may explain qualitatively this behaviour. However, cold nuclear matter effects are poorly constrained at LHC energy and a measurement in p–Pb collisions is necessary to correctly interpret our data in Pb–Pb. The  $J/\psi$  in the dielectron channel measurement is challenging with the present statistics and the large hadronic background. The central to peripheral nuclear modification factor was evaluated [7]. Finally, few tens of exclusive  $J/\psi$  candidate were seen in ultra-peripheral collisions and cross section determination is ongoing.

## 5 Conclusions

Measurements of  $J/\psi$  production have been presented at  $\sqrt{s}=2.76$  and 7 TeV in pp and at  $\sqrt{s_{NN}}=2.76$  TeV in Pb–Pb collisions. In pp collisions, the cross sections are found in good agreement with other LHC data and are used as a baseline for Pb–Pb measurements. In Pb–Pb collisions, the nuclear modification factor results in no significant centrality dependence with less suppression than the one observed at RHIC for the most central collisions.

## References

- [1] T. Matsui and H.Satz, Phys. Lett. **B178**, 416 (1986).
- [2] B. Svetitsky, Phys. Rev. **D37**, 2484 (1988).
- [3] R. Arnaldi (NA60 Coll.), Nucl. Phys. **A 830**, 345c (2009), A. Adare *et al.* (PHENIX Coll.), Phys. Rev. Lett. 98, 232301 (2007).
- [4] J. Wessels, these Proceedings.
- [5] L. Ramello, these Proceedings.
- [6] K. Aamodt *et al.* (ALICE Coll.), arXiv:1105.0380, to be publ. in Phys. Lett. B.
- [7] G. Martinez (ALICE Coll.), arXiv:1106.5889.
- [8] A. Toia (ALICE Coll.), arXiv:1107.1973.